Proceedings of the 23rd International Conference on Lightning Protection (ICLP'96), Firenze, Italy, 23-27 September 1996, Paper 5.15, pp. 585-590.

COMPUTER SIMULATION OF TRANSIENT GROUND POTENTIAL RISE IN LARGE EARTHING SYSTEMS

Leonid D. Grcev[1)] and Markus Heimbach[2)]
[1)] University "St. Cyril and Methodius", Skopje, Republic of Macedonia
[2)] Technical University of Aachen, Aachen, Germany

Abstract - This paper describes a computer model for simulation of TGPR in large substations earthing systems in case of lightning. The earthing system is first modeled by rigorous electromagnetic field theory approach, taking into account the frequency-dependence. Then the model is interfaced to the EMTP, taking into account the interaction between the electric power network and the earthing system. Finally, results of the EMTP analysis are utilized for detailed evaluation of the TGPR as time-domain three-dimensional function. Paper also presents: computer model validation, detailed parametric analysis and an example of practical lightning protection study.

1. Introduction

Lightning protection and electromagnetic compatibility (EMC) studies of electric power installations usually require knowledge of the highest possible elevation of the voltage between the grounding system and the remote neutral earth, that is, "the Ground Potential Rise" (GPR). At power frequency the GPR is a single number, since the grounding systems are usually assumed equipotential [1]. However, in case of lighting or abnormal power system operation, the Transient Ground Potential Rise (TGPR) is a complex three-dimensional time-domain function [2].

This paper describes recent advances in computer simulation of TGPR in large earthing systems.

The first step in the analysis is evaluation of the transient behavior of the earthing system itself. Such analysis was often performed using circuit theory concepts, for example in [3]–[6]. However, all these approaches are based on quasi-static approximation and their validity may be limited to some upper frequency which depends on the size of the grounding system and the electrical characteristics of the earth [7]. More recently, rigorous formulations derived from the full set of the Maxwell's equations have been used in [8], [9] and [2].

The second step of the analysis is to model grounding system as a part of the electric power network. The widely used the EMTP provides proven models for a large number of power system components but not detailed models of grounding systems. The electromagnetic field approach to earthing systems analysis [2] was interfaced to the EMTP in [10], taking into account the frequency-dependent properties and mutual electromagnetic interactions between parts of the earthing system.

This paper includes:

- brief description of the underlying computational methodology ([2], [10]),
- validation of the computer model by comparison with measurements and previously published results,
- detailed parametric analysis that identify parameters with dominant influence on TGPR,
- example of a practical lightning protection study,
- application of computer animation in the evaluation of the TGPR as a time-domain three-dimensional function.

2. Analysis in Frequency-Domain

2.1 Longitudinal Currents in Grounded Structures

The problem is first solved in frequency-domain. The grounding system is assumed to be a network of thin straight cylindrical metallic conductors with arbitrary orientation and finite conductivity. The soil is modeled as linear and homogeneous half-space characterized by conductivity, permittivity and permeability constants.

The first step is to compute the current distribution, as a response to injected current at arbitrary points on the conductor network. First, the conductor network is divided into a number of fictitious smaller segments, Fig. 1. Total current in the conductors $I(\ell)$ is approximated as a linear combination of M sinusoidal expansion functions $F_k(\ell)$, Fig. 1 [11]:

$$I(\ell) = \sum_{k=0}^{M} I_k F_k(\ell) \tag{1}$$

where I_k are unknown current samples.

Longitudinal current distribution (1) may be evaluated from the system of equations:

$$[Z]\cdot[I] = [V] \tag{2}$$

where the elements of the column matrix [I] are unknown current samples. Elements of [Z] are generalized impedances between segments, that take into account all electromagnetic interactions. Elements of [V] are related to the excitation of the system.

To evaluate elements of [Z] (2), rigorous formulas [12] for the electric field are used. The derivation of these formulas is given also in [6]. The influence of the earth's surface is taken into account by the modified image theory [13].

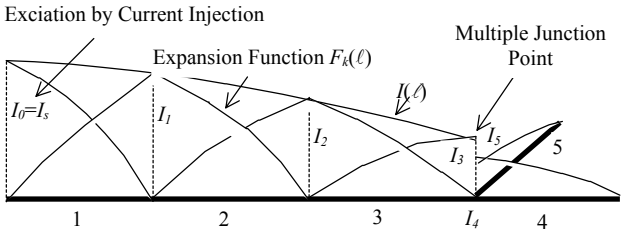

Fig. 1. Approximation of Current Along Segmented Conductor Network.

2.2 Frequency-Dependent Impedances of Earthing Systems

The frequency-dependent impedance of a grounding system is defined as:

$$Z_{mn}(j\omega) = \frac{V_{mn}(j\omega)}{I_n(j\omega)} \tag{3}$$

where $V_{mn}(j\omega)$ denotes the GPR at point m as response to current injection $I_n(j\omega)$ at point n. $Z_{nn}(j\omega)$ is self impedance of the grounding system related to a certain point n, whereas $Z_{mn}(j\omega)$ $(m \neq n)$ stands for the mutual impedance between two points m and n.

When current distribution (1) is known then $V_{mn}(j\omega)$ can be straightforwardly computed [2]. Examples of computed self impedances of 60 x 60 m^2 ground grids are given in Fig. 2.

3. Analysis in Time-Domain

The strength of the presented method is that an arbitrary number of feeding points can be taken into account. In case of J connections between the grounding system and the live parts of the connected electrical network, the impact of the grounding system can be described in frequency domain by the following set of equations:

$$\begin{bmatrix} V_1(j\omega) \\ V_2(j\omega) \\ \cdots\cdots \\ V_J(j\omega) \end{bmatrix} = \begin{bmatrix} Z_{11}(j\omega)\, Z_{12}(j\omega) \ldots Z_{1J}(j\omega) \\ Z_{21}(j\omega)\, Z_{22}(j\omega) \ldots Z_{2J}(j\omega) \\ \cdots\cdots \\ Z_{J1}(j\omega)\, Z_{J2}(j\omega) \ldots\ Z_{JJ}(j\omega) \end{bmatrix} \cdot \begin{bmatrix} I_1(j\omega) \\ I_2(j\omega) \\ \cdots\cdots \\ I_J(j\omega) \end{bmatrix} \tag{4}$$

In transient analyses, however, it is necessary to simulate each element of the electric power system in time-domain. The following technique for rational function approximation permits both the transformation of the frequency-dependent grounding system impedances in time-domain and the interfacing with the EMTP.

In order to incorporate self and mutual impedances into the EMTP the magnitude functions of the impedances are approximated by rational functions of the following form:

$$Z_{mn}(s) \approx Z_{mn,fit}(s) = K \cdot \frac{\prod_{m=1}^{M}(s+z_m)}{\prod_{n=1}^{N}(s+p_n)} = q_0 + \sum_{n=1}^{N} \frac{q_n}{s+p_n} \tag{5}$$

The adaptation of Bode's asymptotic technique

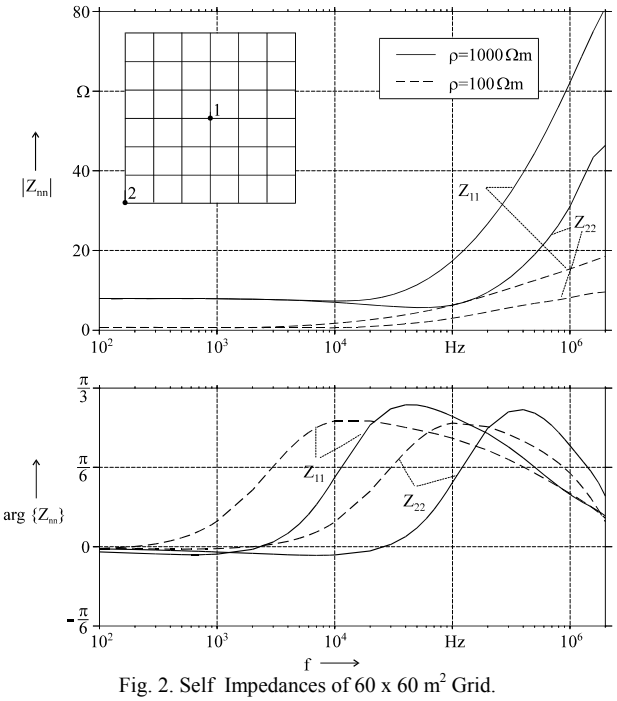

Fig. 2. Self Impedances of 60 x 60 m^2 Grid.

[14] to the highly frequency-dependent parameters of grounding structures was carried out in [6]. A succeeding optimization loop was introduced by the authors in [10] to reduce the deviation. Using this algorithm a system described by (5) is stable and minimum-phase-shift [15].

Mutual impedances $Z_{mn}(\mathrm{j}\omega)$, however, are non minimum-phase-shift functions. $Z_{mn}(\mathrm{j}\omega)$ can be split up into the corresponding minimum-phase-shift function $Z^0{}_{mn}(\mathrm{j}\omega)$ and an all-pass filter A(jω):

$$Z_{mn}(j\omega) = Z^0_{mn}(j\omega) \cdot A(j\omega), \quad A(j\omega) = e^{-j\omega\tau} \tag{6}$$

Due to the shifting property of the Fourier-transform, in time domain (6) is given by

$$z_{mn}(t) \approx z^0_{mn}(t-\tau) \tag{7}$$

where τ denotes the traveling time (delay time) of the fastest frequency response. The traveling time τ results from the finite propagation velocity of the electromagnetic waves between points n and m of the grounding system. In contrast to mutual impedances where injected current and evoked voltage are simulated at different positions of the grounding system the self impedances are minimum-phase-shift functions, since injected current and evoked voltage are simulated at the same position.

Approximating the magnitude function of self impedances, i.e. minimum-phase-shift functions, by means of rational functions according to (5), the phase function is given automatically due to the unambiguous relation between magnitude and phase function. Investigating mutual impedances, i.e. non minimum-phase-shift functions, the procedure results in an approximation of the corresponding minimum-phase-shift function. Hence, in order to simulate the mutual impedances taking into account the time shift

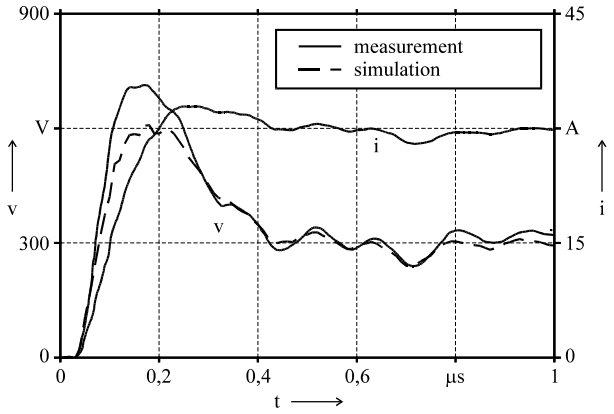

Fig. 3. Comparison with Measurements [16].

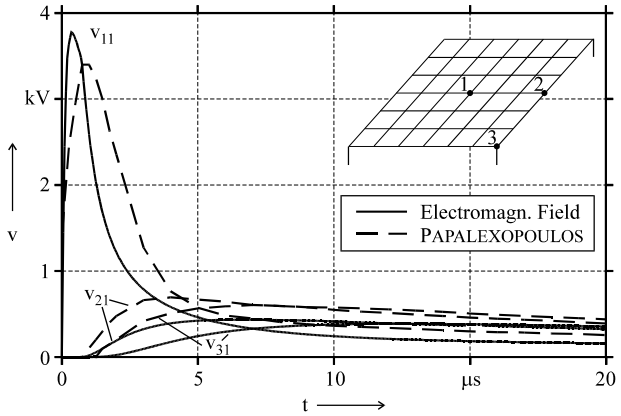

Fig. 4. Comparison with [5] and [17].

in time domain simulation the output signal has to be delayed by the traveling time τ; τ can be determined by comparison of the phase functions of the original (non minimum-phase-shift) $Z^0_{mn}(j\omega)$ and the approximated (minimum-phase-shift) function $Z^0_{mn,fit}(j\omega)$ according to (6):

$$\arg\{Z_{mn}(j\omega)\} = \arg\{Z^0_{mn,fit}(j\omega)\} - \omega\tau \qquad (8)$$

After the approximation procedure self and mutual impedances are passed to the EMTP. Within the EMTP inherent models are used for time domain representation [10], using techniques that reduce the numerical simulation effort drastically.

4. Comparison with Measurements and with Previously Published Results

Measurements of TGPR of a horizontal copper conductor of 8 m length and a 12 mm diameter were available to validate the model. The conductor was buried in a depth of 0.6 m in soil with a specific resistivity of 60 Ωm. The current was fed into one end of the conductor. The voltage to remote ground was measured using a 60 m resistive divider with a bandwidth of 3 MHz. Field measurements were performed by the Electricite de France [16]. Fig. 3 presents the results of the comparisons. The simulated voltages are in good agreement with experiment. The deviation for higher frequencies was found in all other comparisons [6,2] and is related to the inductive voltage drop along the divider for very high frequencies.

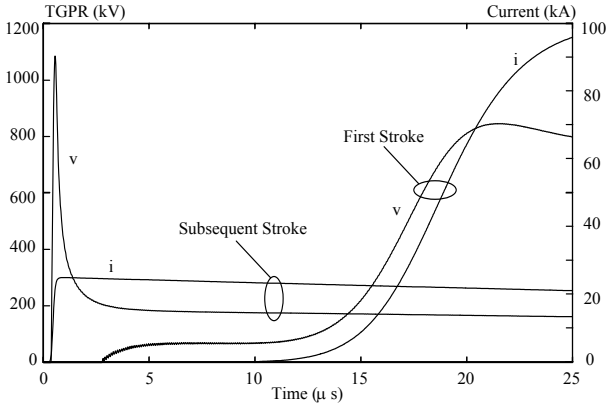

Fig. 5. Influence of Lightning Wave Form.

Fig. 4 presents comparison with a transmission line approach published by Papalexopoulos and Meliopoulos [5,17]. TGPRs are computed at the feed point 1, middle side point 2 and corner point 3 of the 60 m x 60 m grid, at which corners vertical ground rods with a length of 10 m are driven into the ground. The grid is buried at 0.6 m depth in soil with ρ = 100 Ωm. The impulse current with a crest value of 1 kA and an impulse shape of (1/20 µs) is fed into the middle point 1 of the grid. Both approaches simulate maximum TGPR at the feed point in good agreement, with small shift in time. Additionally, [5] overestimates the transient voltage at the remote points, which may be related to the neglect of mutual electromagnetic interactions between parts of the system in [5].

5. Parametric Analysis

Several ground grids are adopted for computations with dimensions varying from 10 x 10 m^2 to 120 x 120 m^2 and with number of meshes from 4 to 124. All are constructed of copper conductors with diameter 1.4 cm and buried at 0.5 m depth. Two types of homogeneous soil are considered: with resistivity 1000 Ωm and relative permittivity 9 ("dry soil") and with resistivity 100 Ωm and relative permittivity 36 ("wet soil"), the same as previously chosen in [4].

The following current wave forms are used:

- the first stroke 100 kA 10/350 µs, and
- the subsequent stroke 25 kA 0.25/100 µs,

defined in [19].

Fig. 5 shows the TGPR at feed point at the corner of 60 x 60 m^2 grid in soil with ρ = 1000 Ωm for the two current wave shapes. Large TGPR is developed for current impulses with short rise time (subsequent stroke). Its peak value is more than five times larger than for power frequency, but the impulse is of short duration (a few microseconds). Consequently, 25 kA subsequent stroke leads to larger TGPR, than 100 kA direct stoke but only for very short time.

The influence of soil conductivity and location of

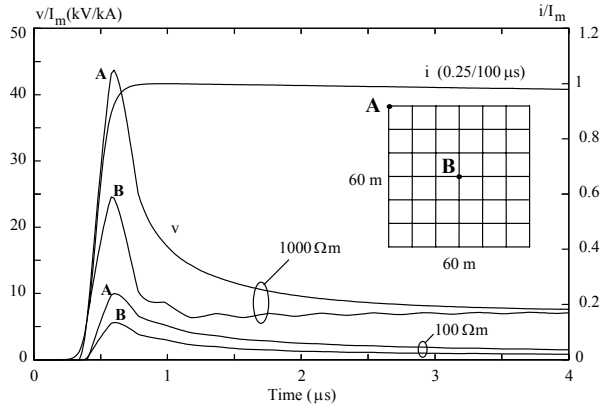

Fig. 6. Influence of Soil Resistivity and Location of Feed Point.

the feed point on the TGPR, as response to subsequent stroke impulse, is shown in Fig. 6. The TGPR is normalized to the maximum of the lightning current impulse I_m.

It can be seen that TGPR is proportional to soil resistivity at longer duration, while the sensitivity is reduced to about 40% for the frontal amplitude. Also as TGPR is becoming larger in poorly conductive soil, the transient period is becoming shorter, due to larger velocity of propagation of electromagnetic pulses. The maximal variation of the TGPR with different locations of the feed point is approximately 1:2, with largest peak values at the corner and smallest at the center of the grid.

Fig. 7 shows the influence of the earthing grid size on the TGPR at the corner feed point. The grid size has large influence on TGPR after the transient period, that lasts for a few microseconds, but has small influence during the transient period. Results indicate that in the range of the maximum TGPR the effective area of the grid is very small. For the analyzed cases it may be approximated as not much greater than about 10 x 10 m^2.

Fig. 8 shows that smaller conductor separation can be used to reduce the TGPR, but only if meshes are substantially smaller that the effective area of the grid. It can be seen in Fig. 8, that among the analyzed cases, only grid with 3 m^2 square meshes, in the effective area near the corner feed point, substantially reduces the maximal TGPR [18].

6. Transient GPR in a 123 kV Substation Subjected to a Lightning Surge Current

A lightning protection study of a 123 kV substation focusing on the TGPR is performed in this chapter. During the transient period mutual coupling between the grounding system and the connected aboveground structures has to be taken into account. In the following the above presented EMTP-based approach is chosen in order to carry out the study.

The grounding system of the investigated substation consists of a 60 x 60 m^2 grid with 6 x 6 meshes, Fig. 9. The copper conductors have a diameter of 14 mm and are buried in a depth of 0.5 m. In order to

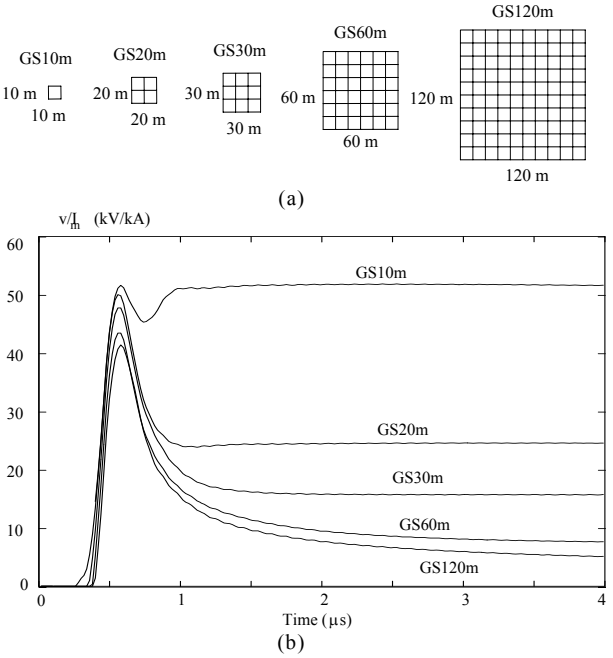

Fig. 7. Influence of Earthing Grid Size (ρ = 1000 Ωm).

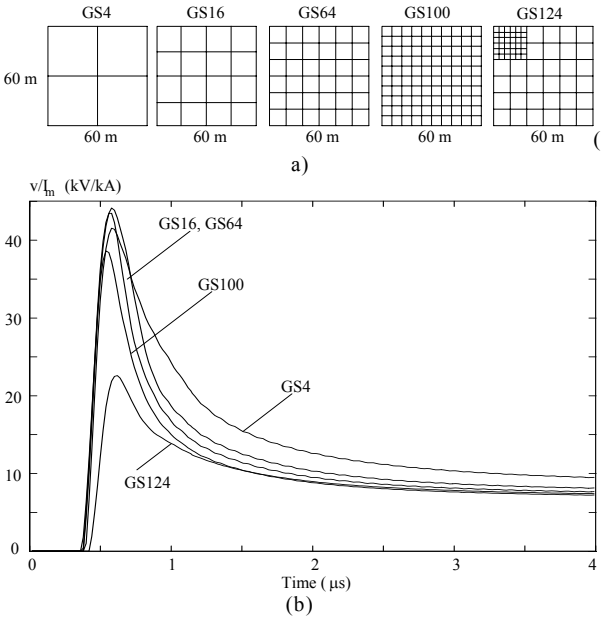

Fig. 8. Influence of Earthing Grid Conductor Separation (ρ = 1000 Ωm).

investigate the influence of the soil parameters on the resulting transients this arrangement is simulated for two different sets of soil parameters given in Section 5. The aboveground electrical components of the substation (voltage transformer, busbar, arrester, and power transformer), as well as the connected overhead transmission line, are modeled within the EMTP and connected to the grounding structure.

A direct lightning stroke hits one phase of the overhead transmission line 300 m before the substation at the phase voltage zero. The lightning stroke has a crest value of -3 kA and an impulse shape

(1.2/50 μs). For usual values of the characteristic impedance ($Z_C \approx 370\ \Omega$) a voltage crest value of about 550 kV is expected. It is assumed that a flash-over to towers does not occur.

The computed currents injected into the grounding system due to the lightning stroke at the arrester's and the transformer's connection to the grounding system are displayed in Fig. 10, for both sets of soil parameters. After 10 μs the currents approach their DC-distribution. The first transients last the longer the higher soil conductivity is. Additionally both sets of soil parameters produce different transient frequencies: $f \approx 650$ kHz in case of $\rho_E = 100\ \Omega$m and $f \approx 570$ kHz in case of $\rho_E = 1000\ \Omega$m, respectively. Comparing self impedances at the feeding points for different soil conductivities (Fig. 2) it becomes obvious, that for the same grid the imaginary (inductive) part of the self impedances is greater for poorly conductive soil. This means, that the resulting inductivity of the circuit consisting of the surge capacity of the transformer, the inductivity of the busbar and the self impedance of the grounding system related to both feeding points for greater for poorly conductive soil leading to smaller natural frequency of the resulting RLC-circuit. The impact of the coupling between the feeding points, can be neglected in a first approximation due to the limited effective area in the frequency range of the transients.

Fig. 11 presents TGPR at the arrester and transformer connections to the earthing system. Their oscillation is damped toward the even dc distribution, but is mutually in counter-phase. This results in large potential difference $\Delta\phi$ (Fig. 11.) between arrester and transformer connection points during the first few oscillations.

Resulting spatial and temporal distribution of the TGPR on the earthing system is very complex and may be observed only by computer animation. Fig. 12 presents several snapshots of the 3D distribution of the TGPR of the ground grid, illustrating the use of computer animation.

7. Conclusions

Paper presents integration of the rigorous model for analysis of transients in complex and spacious earthing systems, based on electromagnetic field theory approach, with the EMTP. Advantage of this approach is that frequency dependence and electromagnetic interactions between the parts of the system are rigorously modeled together with the interactions between the earthing system and various components of the power network. This enables computations of overvoltages throughout the electric power system and detailed analysis of the TGPR of large substation earthing system.

Presented parametric analysis confirm known facts that large in magnitude, but with short duration, TGPR are developed when the ground grid is subjected to fast rising current impulse, similar to typical subsequent stroke of lightning. The resulting TGPR is larger for poorly conductive soil and for stroke near the edge of the grid. The parametric analysis also reveals that the effective area of the grid during the transient period is very small. Important conclusion is that reduction of the TGPR is possible with smaller conductor separation in the effective area of the grid around points where lightning protection system is connected to the earthing system.

The practical example of a lighting protection study of 123 kV substation reveals that the resulting TGPR in the ground grid is very complex three-dimensional time-domain function. It is demonstrated that very helpful tool for analysis of such complex transient behavior is computer animation of 3D perspectives of the TGPR.

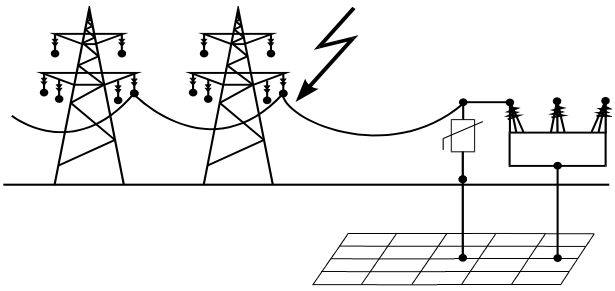

Fig. 9. Lightning Protection Study of a 123 kV Substation.

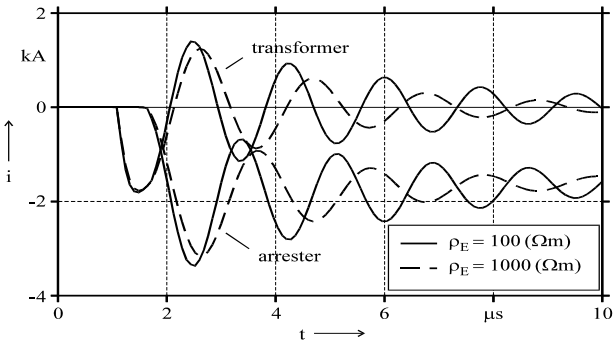

Fig. 10. Injected Current into the Earthing System.

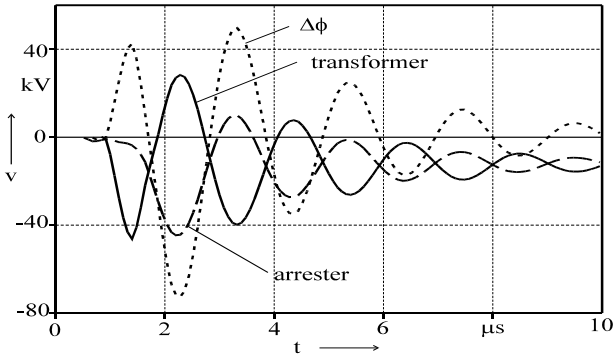

Fig. 11. TGPR at the Arrester and Transformer Connections and the Potential Difference.

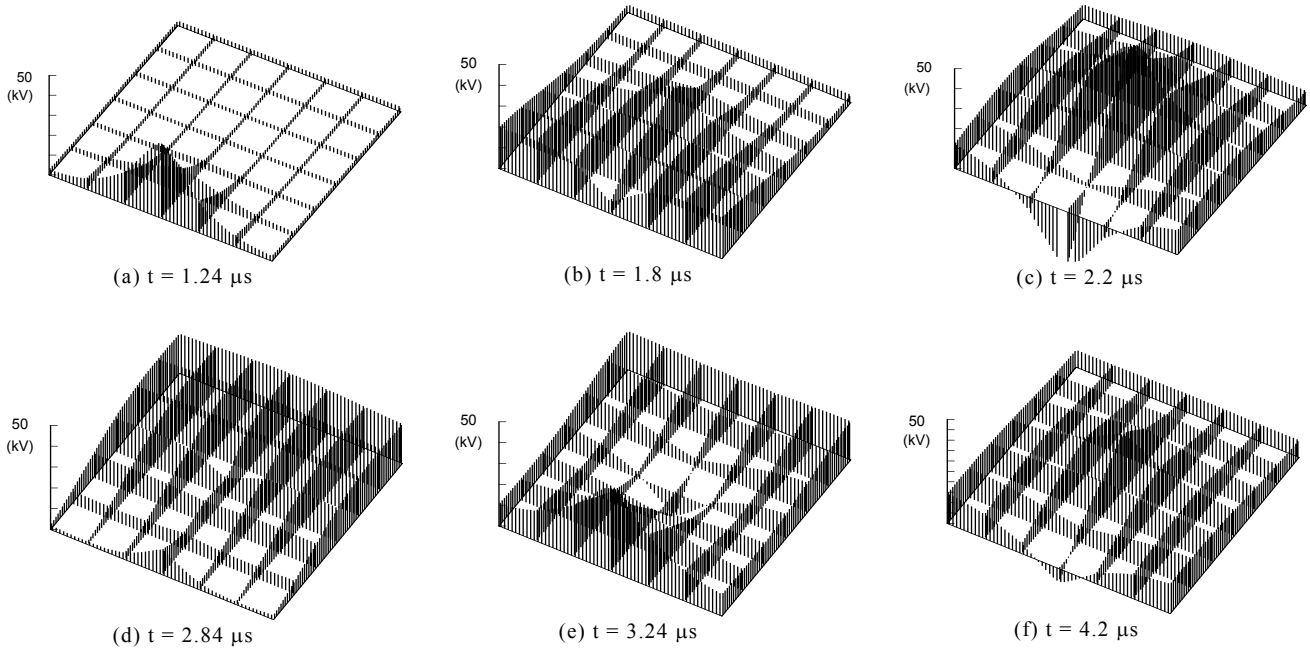

Fig. 12. Snapshots of Computer Animation of TGPR of 60 x 60 m^2 Ground Grid in an 123 kV Substation.

8. Acknowledgment

The work was partially supported by a German-Macedonian project. The first author acknowledges partial support by the Ministry of Science of Republic of Macedonia.

9. References

[1] *IEEE Guide for Safety in AC Substation Grounding*, New York: IEEE, 1986, (ANSI/IEEE Std. 80-1986).

[2] L. Grcev, "Computer Analysis of Transient Voltages in Large Grounding Systems," to be published in *IEEE Transactions on Power Delivery* (IEEE Paper 95 SM 363-2 PWRD).

[3] M. Ramamoorty, M. M. B. Narayanan, S. Parameswaran, and D. Mukhedkar, "Transient Performance of Grounding Grids," *IEEE Transactions on Power Delivery*, Vol. PWRD-4, Oct. 1989, pp. 2053-2059.

[4] A. P. Meliopoulos and M. G. Moharam, "Transient Analysis of Grounding Systems," *IEEE Transactions on Power Apparatus and Systems*, Vol. PAS-102, Feb. 1983, pp. 389-399.

[5] A. D. Papalexopoulos and A. P. Meliopoulos, "Frequency Dependent Characteristics of Grounding Systems," *IEEE Transactions on Power Delivery*, Vol. PWRD-2, October 1987, pp. 1073-1081.

[6] F. Menter and L. Grcev, "EMTP-Based Model for Grounding System Analysis," *IEEE Transactions on Power Delivery*, Vol. 9, October 1994, pp. 1838-1849.

[7] R. G. Olsen and M. C. Willis, "A Comparison of Exact and Quasi-Static Methods for Evaluating Grounding Systems at High Frequencies," to be published in *IEEE Transactions on Power Delivery* (IEEE Paper 95 SM 395-4 PWRD).

[8] L. Grcev, *Computation of Grounding Systems Transient Impedance*, Ph. D. Thesis, University of Zagreb, Croatia (formerly Yugoslavia), 1986.

[9] L. Grcev and F. Dawalibi, "An Electromagnetic Model for Transients in Grounding Systems," *IEEE Transactions on Power Delivery*, Vol. PWRD-5, No. 4, October 1990, pp. 1773-1781.

[10] M. Heimbach and L. Grcev, "Grounding System Analysis in Transients Programs Applying Electromagnetic Field Approach," to be published in *IEEE Transaction on Power Delivery*.

[11] J. H. Richmond, "Radiation and Scattering by Thin-Wire Structures in the Complex Frequency Domain," in *Computational Electromagnetics*, E. K. Miller, Ed., New York: IEEE Press, 1992.

[12] S. A. Schelkunoff, H. T. Friis, "Antennas, Theory and Practice", New York: Wiley, 1952, p. 401.

[13] T. Takashima, T. Nakae, and R. Ishibashi, "Calculation of Complex Fields in Conducting Media," *IEEE Transactions on Electrical Insulation*, Vol. 15, 1980, pp. 1-7.

[14] H. W. Bode, "Network Analysis and Feedback Amplifier Design", New York: Van Nostrand,1945.

[15] A. Papoulis, "The Fourier Integral and its Application", New York: McGraw-Hill, pp. 204-217.

[16] H. Rochereau, "Response of Earth Electrodes when Fast Fronted Currents are Flowing Out", *EDF Bulletin de la Direction des Etudes et Recherches*, serie B, no. 2, 1988, pp. 13-22.

[17] A. D. Papalexopoulos, "Modeling Techniques for Power System Grounding Systems", Ph. D. dissertation, Georgia Institute of Technology, Georgia, 1985.

[18] L. Grcev and M. Heimbach, "Frequency Dependent and Transient Characteristics of Substation Grounding Systems," to be published in *IEEE Transactions on Power Delivery*.

[19] IEC 1312-1, *Protection Against Lightning Electromagnetic Impulse. Part 1: General Principles*, 1995.